Chen, X. and Chen, Q. 2010. "Comparison of different delivery methods for sterilizing unoccupied commercial airliner cabins," *Building and Environment*, 45(9), 2027-2034.

Comparison of Different Decontaminant Delivery Methods for Sterilizing Unoccupied Commercial Airliner Cabins

Xi Chen[1], and Qingyan Chen[1 *]

National Air Transport Center of Excellence for Research in the Intermodal Transport Environment (RITE), School of Mechanical Engineering, Purdue University, West Lafayette, Indiana, USA[1]

Abstract

Effective decontamination is crucial if an airliner cabin is contaminated by biological contaminants, such as infectious disease viruses or intentionally released biological agents. This study used computational fluid dynamics (CFD) method as a tool and vaporized hydrogen peroxide (VHP) as an exemplary decontaminant and *Geobacillus stearothermophilus* spores as a simulant contaminant to investigate three VHP delivery methods for sterilizing two different airliner cabins. The CFD first determined the airflow and the transient distributions of the contaminant and decontaminant in cabins. Auxiliary equations were implemented into the CFD model for evaluating efficacy of the sterilization process. The improved CFD model was validated by the measured airflow and simulated contaminant distributions obtained from a cabin mockup and the measured efficacy data from the literature. The three decontaminant delivery methods were (1) to supply the mixed VHP and air through the environmental control system of a cabin, (2) to send mixed VHP and air through a front door and to extract them from a back door of a cabin, and (3) to send directly VHP to a cabin and enhance the mixing with air in the cabin by fans. The two air cabins studied were a single-aisle and a twin-aisle airliner one. The results show that the second decontaminant delivery method (displacement method) was the best because the VHP distributions in the cabins were most uniform, the sterilization time was moderate, and the corrosion risk was low. The method displaced the existing air by the air/disinfectant solution, rather than dispersive mixing as the other two methods.

1. Introduction

When an airliner cabin is contaminated by biological contaminants, such infectious disease viruses or intentionally released biological agents, it needs to be quickly decontaminated before it can be returned in to service. Effective decontamination can reduce the risk of infection for passengers and crew members to be boarded. To reduce the possible flight delay and cancellation, efficient decontamination is crucial if all the aircraft should be routinely decontaminated during an infectious disease outbreak. It is therefore important to develop viable decontamination methods that are effective in killing the viruses or biological agents, easy to use, fast in decontamination process, and safe for returning the aircraft to service after the decontamination.

There are a range of decontamination methods being used in enclosed spaces for both military and civil applications. Many use lights for disinfection, such as photocatalysis [3, 22], ultraviolet light [4, 10, 12] and X-rays [12]. Some liquid chemical agents are also used as decontaminants, such as L-Gel for chemical and biological warfare agents in military use [12], and alcohol [12], phenol [12], and hydrogen peroxide (H_2O_2) [12] in civil applications. Although liquid hydrogen peroxide is popular for disinfecting a wide range of organisms [1], it is relatively

* Corresponding author. Mailing address: 585 Purdue Mall, West Lafayette, IN 47905. Phone: (765)496-7562, Fax: (765)494-0539. E-mail: yanchen@purdue.edu.

new to use vaporized hydrogen peroxide (VHP) as a gaseous decontaminant [6]. The disinfection capacity of VHP has been under investigation for various applications like freeze dryer [7], ultracentrifuge [8], dental instruments [13], biological safety cabinets [17], and rooms [17], etc. Compared with other gas decontaminants, e.g., formaldehyde and ethylene oxide, the VHP is a less toxic and safer alternative to release in the air in occupied spaces [2]. The final product of VHP after decontamination process is oxygen and water. If used properly, the VHP is environmental friendly. Thereby, VHP has a great potential for decontamination in enclosed surfaces and human occupied environments.

VHP for aircraft cabin decontamination has been investigated by both experimental and numerical methods. Shaffstall et al. [16] conducted a study of the decontamination performance of the VHP in a section of aircraft cabin and concluded that their VHP delivery system was working. Shaffstall et al. also built a Computational Fluid Dynamics (CFD) model for this cabin section and validated the model by the experimental data. However, they did not explore different decontaminant delivery methods for various airliner cabins. This study would further study the problem by using three VHP delivery methods to decontaminate two different cabins aiming to develop an optimal method.

2. Methods

2.1 Numerical method

In order to find an optimal decontamination method, this study used the CFD technique based on the Reynolds averaged Navier-Stokes (RANS) equations with the Renormalize Group k-ε (RNG k-ε) model to calculate the distributions of air velocity and species concentrations. The governing transport equations can be expressed in the following form:

$$\rho\frac{\partial\phi}{\partial t}+\rho U_j\frac{\partial\phi}{\partial x_j}-\frac{\partial}{\partial x_j}\left[\Gamma_{\phi,\mathrm{eff}}\frac{\partial\phi}{\partial x_j}\right]=S_\phi \qquad (1)$$

where ϕ represents Reynolds averaged variables, U the mean velocity, t the time, x the coordinate, $\Gamma_{\phi,\mathrm{eff}}$ the effective diffusion coefficient, and S_ϕ the source term. The Reynolds averaged variables for the present study includes three velocity components U_j, turbulence kinetic energy k and its dissipation rate ε, and contaminant and decontaminant concentrations C. Equation (1) also represents the mass conservation when ϕ equals unit.

The CFD can calculate the distributions of air velocity and species concentrations in different air cabins. It is essential to implement decontamination process into the CFD so that the model can be used to identify an optimal decontamination method. Typically decontamination process consists of three phases: dehumidification, sterilization, and aeration. A detailed description of each phase can be referred to [2]. The objectives of the dehumidification and aeration are relatively easy to reach. The main focus of this investigation was on the sterilization to determine efficacy of the sterilization process. During sterilization, the VHP concentration should be higher than 80-100 ppm to be effective but lower than 2000 ppm [5] to avoid condensation in the cabin because condensed hydrogen peroxide is highly toxic and can cause avionics corrosion. Ideally, the VHP concentration should be between 100 and 1000 ppm.

In order to enable the CFD to calculate the time-dependent distributions of infectious disease viruses or biological agents and the efficacy of the sterilization process, this study simply assumed the viruses or agents were an airborne contaminant. If the infectious disease viruses or biological agents are generated from coughing, sneezing, talking and breathing of a human being,

the assumption is appropriate [11]. Reference [11] shows that settling time for different size of droplets from human beings. It is true that very large droplets are not airborne and will settle on surfaces, which would not be included in the study. Additional auxiliary equations must be implemented into the CFD to correlate the VHP concentration and the contaminant concentration.

The VHP was naturally decomposed and consumed during the decontamination process. The reduction rate was considered by the half-life time the VHP. The half-life time, subject to exponential decay, is the time required for the VHP quantity to decay to half of its initial value. The time dependent VHP concentration C at location i and time $\tau + \Delta\tau$ can be calculated by the following equation:

$$C(i,\tau+\Delta\tau) = C(i,\tau)\cdot 2^{-\frac{\Delta\tau}{H}} \quad (2)$$

where Δt is the time step and H is the half-life time. Thomas [18] conducted VHP decontamination experiments in airliner cabins, and identified the half life time H to be 30 minutes, which was used for this study.

The survival concentration of infectious disease viruses or biological agents (contaminant concentration), N, was calculated by:

$$\log_{10} N(i,\tau+\Delta\tau) = -A\Delta\tau + \log_{10} N(i,\tau) \quad (3)$$

where i is the location, τ is current time, Δτ is time step. A is the sterilization rate calculated from:

$$A = \frac{1}{60\cdot D} \quad (4)$$

The D value in the equation refers to decimal reduction time, the time required at a certain temperature to kill 90% of the organisms. This study used the D-value obtained by Thomas [18] from the measurement data of the VHP against *Geobacillus stearothermophilus* spores at 30 ºC as shown in Figure 1. The spores used by Thomas were on tri-pack stainless steel coupons. Rogers et al. [14] compared gaseous H P inactivation of B. subtilis, B. anthracis, and G. stearothermophils on a variety of surfaces and found that generally G. stearothermophilus was more resistant than the other organisms. Therefore, this investigation selected G. stearothermophilus.

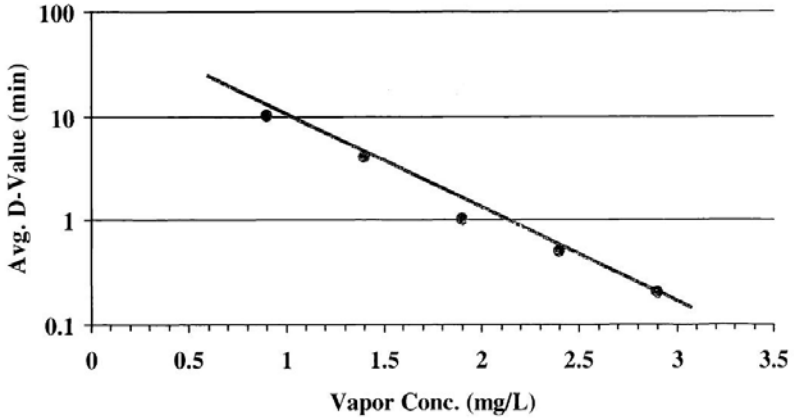

FIG 1. The D-value at 30ºC on *Geobacillus stearothermophilus* spores [18].

The D-value can be calculated accordingly as:

$$\log_{10} D = D_1 \times C + D_2 \quad (5)$$

where C is the local concentration of VHP, in ppm, D_1 = 1149.4, and D_2 =1.954.

With those auxiliary equations, the CFD model can be used to calculate the efficacy of the sterilization process for identifying optimal decontamination method through the flow chart shown in Figure 2.

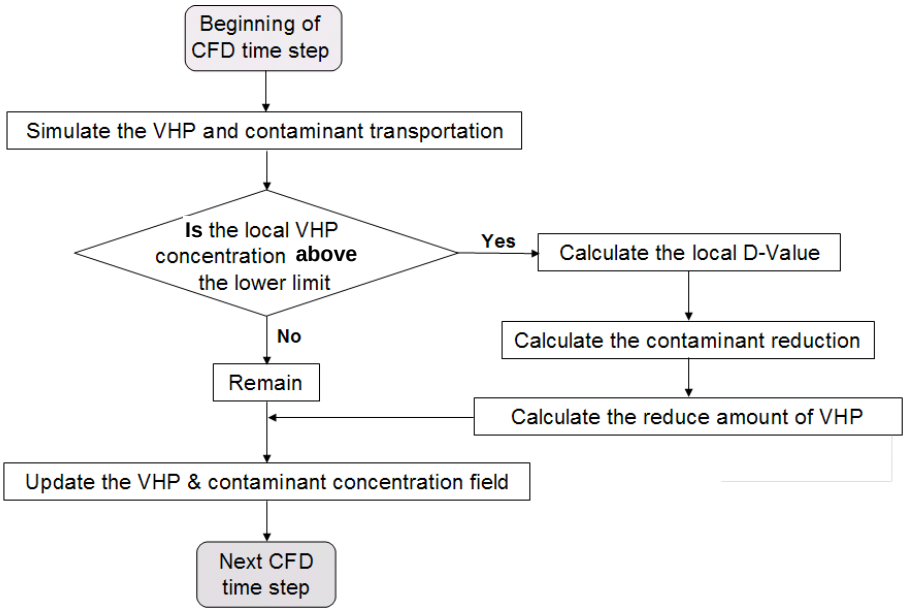

FIG. 2. The flow chart of the sterilization process in the numerical simulation.

2.2 Experimental method

The experimental data for validating the CFD model was obtained in a twin-aisle cabin mockup of a commercial airplane with four rows and 28 seats. Figure 3 shows the schematic and measurement setup inside the cabin mockup. The interior dimensions of the cabin at floor level were 4.9 m (X) × 4.32 m (Y). While the heights of the ceiling varied, the highest ceiling was 2.1 m from the floor. The diffusers on the center of the ceiling discharged supply air into both sides of the cabin with an angle about 30-60 degree downwards from the ceiling. The exhaust outlets were at the bottom of the two side walls above the floor. Several auxiliary fans of 18" × 18" can be operated when needed to help improve the air mixing in the longitudinal direction, because the airflow in the direction was normally minimal. The total airflow rate of from the Environmental Control System (ECS) was 0.23 m^3/s. The airflow rate of each mixing fan was 0.44 m^3/s. To simulate a decontaminant, such as VHP, a tracer gas (SF_6) source was released at the center of the ceiling with a volumetric generation rate of 5×10^{-6} m^3/s with 1% SF_6 solution in air. The tracer gas was released from a sponge material so that it comes out to the air at a negligible velocity around the sponge material.

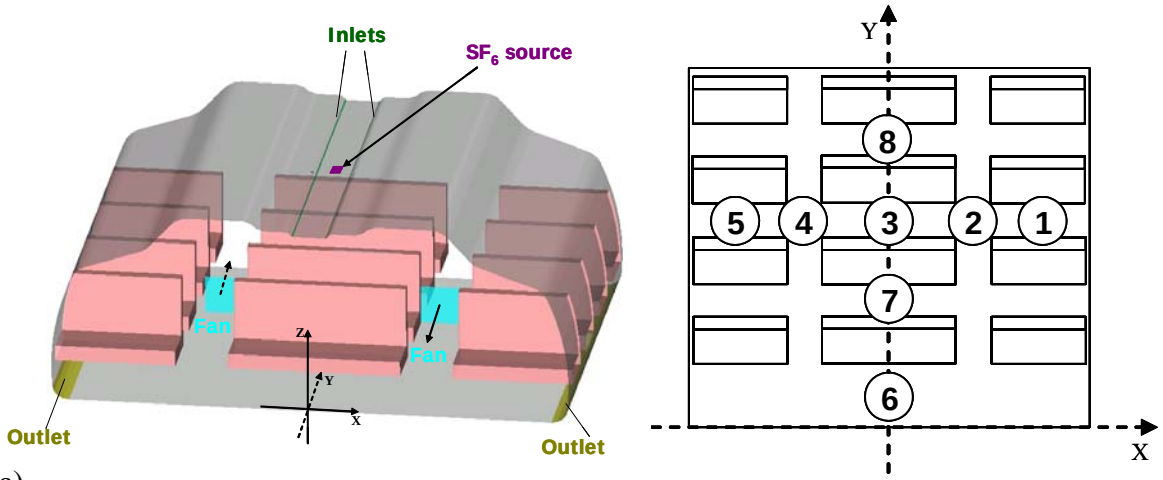

FIG. 3. (a) Sketch of the cabin mockup used in the experiment and CFD simulations and (b) measuring positions for tracer gas concentrations.

The measurements were conducted in both cross sectional and longitudinal directions of the cabin mockup as shown in Figure 3(b). The study used two sets of Kaijo Ultrasonic Anemometer (DA-650) with TR-92T probes to measure the air velocity. The TR-92T anemometer probe had a 3 cm span size. The small span size minimizes the measurement error caused by volume averaging. The accuracy of the anemometers was 0.005 m/s with ±1% error for velocity components. An INNOVA 1312 photo-acoustic multi-gas analyzer and an INNOVA 1309 multi-channel sampler were used to measure and sample the SF_6 concentrations. INNOVA The accuracy of the tracer-gas measurement is 0.1 ppb.

Before taking data, the environmental control system for the cabin was operated for around 48 hours to ensure a stable airflow and temperature distribution. Although accurate measurements of the boundary condition near the air supply inlet were very crucial for CFD simulations, the ultrasonic anemometers were not suitable. The linear diffusers had a width of only 2.5 cm, which was smaller than the sensor span size of the ultrasonic anemometer. This investigation used 16 omni-directional hot-sphere anemometers to obtain air velocity at five different heights close to the diffusers. The 16 hot-sphere anemometers were grouped and attached to a movable frame. The frame was adjustable both horizontally and vertically. A total of 560 points were measured along the two air supply diffusers on the cabin ceiling. Note that the omni-directional anemometers cannot measure air direction. The airflow direction at the diffusers was visualized by a smoke tester and the corresponding jet angles of air supply were recorded. The corresponding jet angles of air supply were estimated in both cross sectional and longitudinal directions. Zhang et al. [21] provided detailed information about the experimental measurements. The boundary conditions at the auxiliary fans were also measured by the ultrasonic anemometers at 16 points in front of each fan.

Since only two anemometers were available, they were moved manually from one location to another in the cabin in order to measure the air velocity distributions. At each location, the anemometer measured the air velocity for at least four minutes at a measuring frequency of 20 Hz (about 4800 readings). When an anemometer was moved from one location to another, the system was stabilized for about 10 minutes so to avoid recording the disturbance caused by moving the sensor. Our experiment shows that it took 30 minutes for the system to become steady after the tracer-gas was injected. Our tracer-gas measurements took about 30

seconds to sample the air. For each location, ten measurements were repeated. The calculated standard deviation was less than 10% of the mean value at most locations except those close to the tracer-gas source with the highest standard deviation of 30% of the mean value.

2.3 Validation of the numerical method

The CFD with RNG k-ε model has been very popular in modeling airflow and contaminant transport in various indoor airflows [15, 19, 20]. However, this does not guarantee the RNG k-ε model is valid for the cabin environment due to its unique flow characteristics, such as highly curved shape, dense furniture, and highly turbulent airflow. Since the auxiliary equations used approximations, it is essential to further validate the CFD model for its ability to determine correctly decontamination efficacy. Due to the practical constraints in obtaining suitable experimental data for the validation, this study used two sets of data: one for validating the CFD model and the other for validating the efficacy of the sterilization process.

Figure 4 shows the comparison of simulated and measured velocity fields with or without the mixing fans in operation. For the case without mixing fans (Figure 4(a)), the main airflow pattern was roughly two dimensional. The numerical model could capture the airflow pattern in the cross sectional plane with remarkable differences. The model well predicted the main circulation on the right, but was less accurate on the left. Since the largest eddy (main circulation) was driven by the air supply jet, the discrepancies could likely come from inaccurate boundary conditions specified at the left supply diffuser. The boundary conditions of air supply jets were crucial in predicting airflow field inside the cabin, since the air jets were the strongest momentum sources in this case.

When the fans were switched on, they generated the highest momentum sources in the cabin. Figure 4(b) shows the simulated flow pattern in a horizontal plane across the auxiliary fans. The numerical results reasonably agreed with experimental data indicating that the fan boundary conditions were accurately specified.

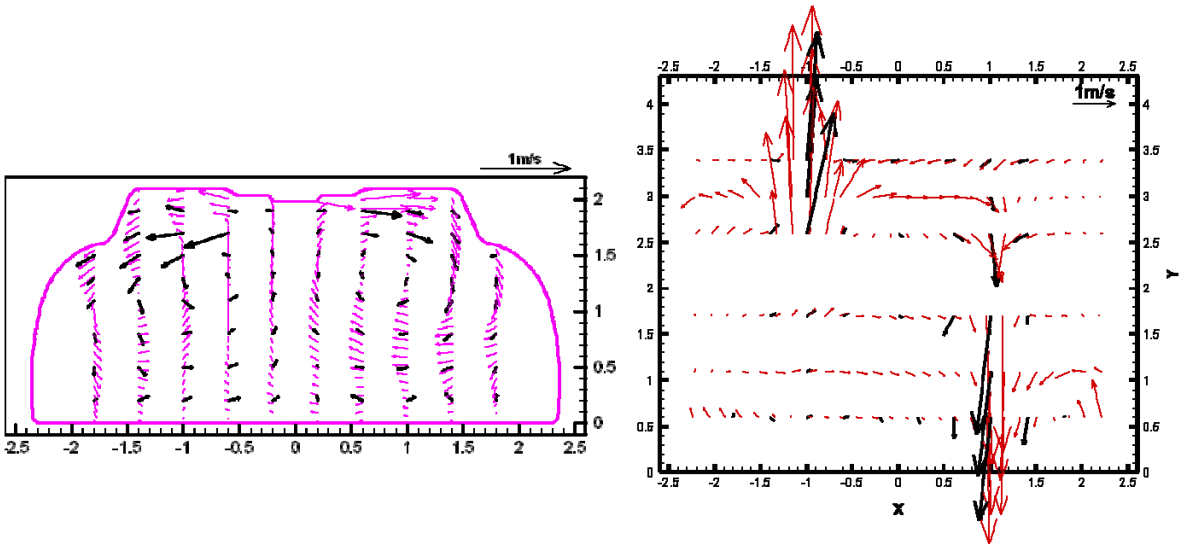

(a) (b)

FIG. 4. Comparison of calculated air velocity with experimental data (bold arrows for experimental data and thin arrows for CFD results) (a) Without fans, cross section between 2nd and 3rd row and (b) With fans, horizontal plane across the center of mixing fans

The calculated and measured tracer-gas concentrations were compared in Figure 5. Due to the limited space available in this paper, only the results for the case with the mixing fans is shown in the figure. The results for the case without the mixing fans were similar. The agreement between the calculation and measurement is reasonable. The relative errors at most positions were smaller than 10-15%, although some larger discrepancies existed in the upper part of position 3. The tracer-gas concentration was very uniform due to the well-mixed airflow.

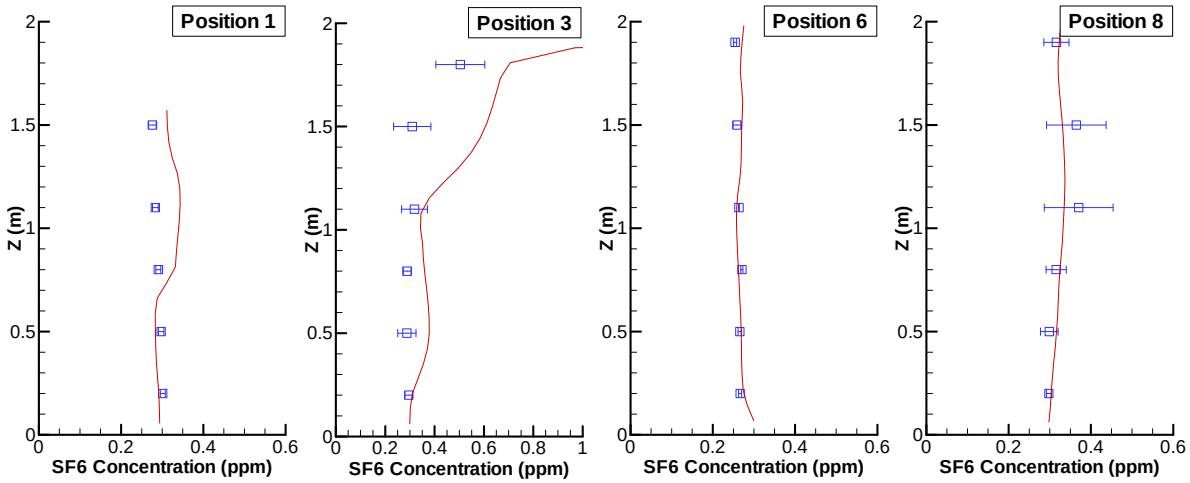

FIG. 5. Comparison of the calculated and measured tracer-gas concentration in selected positions in the cabin (symbols for the measurements and lines for the calculation). Z is the height from the cabin floor.

The comparison between the calculated and measured data above shows differences in some positions. Neither the experiments nor the numerical simulations were free from errors. Considering the application of the CFD model for searching an optimal decontamination method, it is sufficient to capture the main feature of the airflow and tracer-gas concentration distributions in the cabin mockup.

In addition to the airflow and tracer-gas validation of the CFD program by using the experimental data obtained by us above, this study further validated the CFD program for its ability to determine the efficacy of the sterilization process by using the following data from Shaffstall et al. [16]. Shaffstall et al. used biological indicators to evaluate the sterilization efficacy by VHP in a section of a Boeing 747-100 aircraft fuselage in the Aircraft Environmental Research Facility at the Federal Aviation Administration's Civil Aerospace Medical Institute. The cabin segment was 9.75 m long with a volume of approximately 140 m^3 without seats as shown in Figure 6. The test section was separated from the rest of the cabin by two bulkheads built specifically for the test. Tape and plastic sheeting were used throughout the cabin to minimize VHP leakage during the testing.

FIG. 6. Photograph showing the air cabin section used [16].

Their test introduced VHP into the cabin section using four VHP generators (STERIS VHP 1000), located outside of the test area. The generators were completely self-contained bio-decontamination systems with the ability to dehumidify, generate vaporized hydrogen peroxide, and aerate sealed enclosures. The inlets and outlets of the generators passed into the cabin segment through openings in the bulkheads as shown in Figure 7. The decontamination efficacy was measured through the use of biological indicator coupons. Figure 7 also shows the indicator locations labeled from 1 through 39 in 15 positions. Each position has two or three indicators hanged in different heights. The biological indicators were tri-pack stainless steel coupons inoculated with approximately 10^4, 10^5, and 10^6 CFU (Colony Forming Units) with *Geobacillus stearothermophilus* spores packaged in sub-divided Tyvek® envelopes (Apex Laboratories, Inc.).

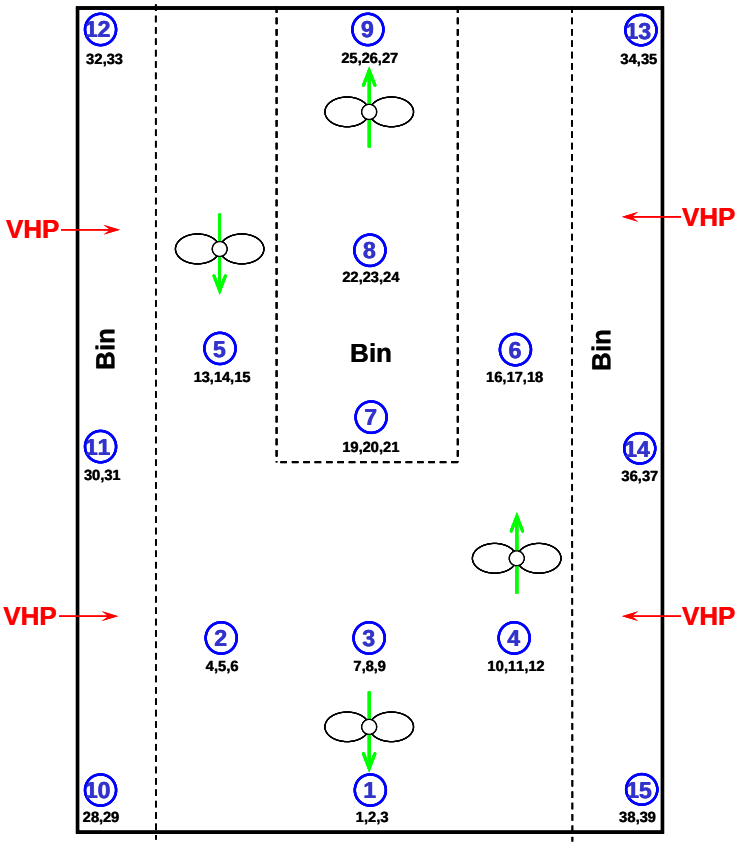

FIG. 7. Cabin section showing locations of the biological indicators, VHP supply inlets, and fans.

Several sets of experimental data were available, but this investigation used only one of them. In this test, the environmental control system was off. The STERIS Model 1000 VHP generators had the capability to recirculate air from the test section of the cabin and this recirculation feature was evaluated in the test. Four oscillating fans were used to assist in the air mixing. The oscillating fans in the measurement were modeled as box fans with a fixed flowing direction in the simulation model. Each fan was running with an airflow rate of 0.9 m^3/s during the test.

Table 1 shows the results from the biological indicators. A reading of small than 10^4 may indicate a four-log biological reduction, while a reading of greater than 10^6 indicates a six-log kill of the *Geobacillus stearothermophilus* spores within the particular biological indicator. Intermediate levels of biological reduction were reported based on the coupon showing no growth, where growth was seen on the next higher-level coupon. Limited by the accuracy of the indicators, the tested results only gave a range of the reduced amount of the contaminant. This table also shows a good agreement of the killed *Geobacillus stearothermophilus* spores by VHP calculated with that tested in most of the positions. Thus the comparison shows that the CFD method is capable to determine the efficacy of the sterilization process.

TABLE 1. Comparison of the calculated and tested results of the reduced *Geobacillus stearothermophilus* spores in the 39 biological indicator positions.

Position	Calculated	Tested	Position	Calculated	Tested
1	9.09×10^5	$>10^6$	21		
2	9.09	$*10^5$	10	^{5}	22
3	9.09×10^5	10^5	23	9.09×10^5	10^5
4	1.45×10^5	10^5	24	9.09×10^5	10^5
5	5.45×10^5	10^5	25	9.09×10^5	10^5
6	7.27×10^5	10^5	26	9.09×10^5	10^5
7	7.27×10^5	10^5	27	9.09×10^5	10^5
8	7.27×10^5	10^5	28	1.64×10^5	10^5
9	9.09×10^5	10^5	29	5.45×10^5	$>10^6$
10	1.82×10^5	10^5	30	1.27×10^5	10^5
11	7.27×10^5	10^5	31	3.64×10^5	$<10^4$
12	7.27×10^5	10^5	32	1.82×10^5	10^5
13	9.09×10^5	10^5	33	7.27×10^5	10^5
14	9.09×10^5	10^5	34	5.45×10^5	10^4
15	9.09×10^5	10^5	35	1.27×10^5	10^5
16	9.09×10^5	10^5	36	3.64×10^5	10^5
17	9.09×10^5	10^5	37	9.09×10^5	10^5
18	9.09×10^5	10^5	38	1.82×10^4	10^4
19	9.09×10^5	10^5	39	5.45×10^5	10^5
20	9.09×10^5	10^5			

The number of the surviving *Geobacillus stearothermophilus* spores is an important criterion for determining the efficacy of the sterilization process. The number should be evaluated spatially and temporally. The spatial evaluation is to check if the concentration of infectious disease viruses or biological agents falls below the required level in an airliner cabin. The temporal evaluation is to assess the time used for sterilization.

The uniformity of VHP is another crucial parameter for evaluating the efficacy. This is because, with a fixed amount of VHP in a cabin, a non-uniform distribution of VHP implies that the VHP concentration could be low in some regions and high in other regions. As a result, the decontamination efficiency could be reduced. If the VHP concentration is too high in some regions, it will increase condensation risk. This investigation calculated the uniformity of VHP concentration by a statistical parameter: the coefficient of variation, $CV_i(t)$, as [9]:

$$CV_i(t) = \frac{1}{\overline{C_i}(t)}\sqrt{\frac{\sum_{i=1}^{N}\left(C_i(t)-\overline{C_i}(t)\right)^2}{N}} \qquad (6)$$

where $\overline{C_i}(t)$ is the volumetric averaged VHP concentration at time = t, $C_i(t)$ is the VHP concentration at each sampling point at time = t, and N is the number of sampling points. Our calculation used the total grid cell number for the CFD as the N.

3. Case Study

This investigation used two different airliner cabins as shown in Figure 8 to find out an optimal decontaminant delivery method. The single-aisle cabin had three rows of first class in front and 25 rows of economy class. The twin-aisle airliner cabin had three rows of first class in front and 30 rows of economy class. The pitch was 0.965 m for the first class and 0.864 m for the economy class. The self-enclosed spaces, i.e., closets, galleys and lavatories, were labeled by C, G and L, respectively. These self-enclosed spaces were not modeled in our calculations.

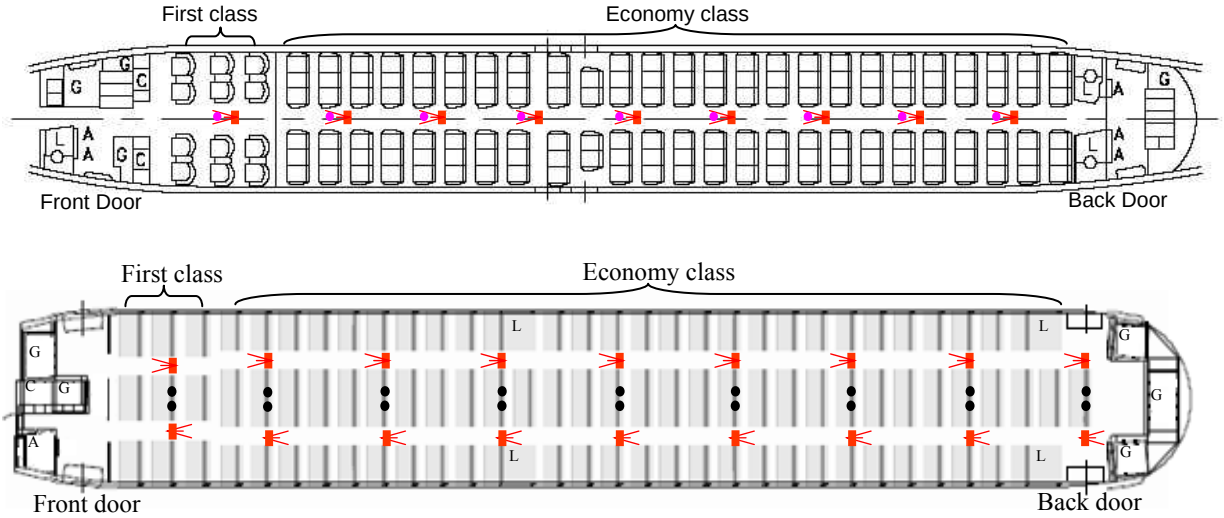

FIG 8. A single-aisle cabin and a twin-aisle cabin used to evaluate different decontaminant delivery methods. The red squares were mixing fans and the arrows indicated airflow directions. The black dots were the VHP delivery positions.

This study compared three different decontaminant delivery methods for each of the cabin. The first method (case A) supplied outside air at 10 L/s per seat and VHP through the ECS. The VHP was premixed with the outdoor air before they were supplied into the cabin so that the VHP concentration at the inlets was uniform. The second method (case B) did not use the ECS. A front door and a back door of the cabin were used as air supply inlet and outlet, respectively. The total outdoor air supplied to the front door was 10 L/s per seat. Thus a displacement flow was developed along the longitudinal direction in the cabin. This method was to use the air/disinfectant solution to displace the existing air in the cabin. The air and VHP were mixed before injecting into the cabin through the front door. The third method (case C) delivered directly the decontaminant into the cabins with the ECS on. In this case, the ECS supplied only 100% outdoor air at 10 L/s per seat. Many auxiliary fans were operated to enhance the mixing of cabin air with the VHP. The black dots in Figure 8 show the VHP delivery locations at a height near the ECS inlets, while the red squares and arrows show the position and direction of the mixing fans which are located on the aisles with the central height 1 m. Please note that the second (displacement) method was different from dispersive mixing as the other two methods. No recirculated air was used in Cases A and C and the ECS was completely shut down in Case B. Since the same ventilation rate was used for all the three cases, the impact of different flow rate was eliminated.

The same VHP supply rate was used for the twin-aisle and single-aisle cabins. The simulation started with a stable and dehumidified airflow field. The contaminant (*Geobacillus stearothermophilus* spores) concentration was 5×10^6 #/m^3. When the mean contaminant concentration in the cabin was below 1000 #/m^3, the sterilization was considered to be completed. Of course, the number of the spores could vary from case to case, the above assessment in fact used a three-log reduction as a criterion for disinfection.

Figure 9 shows the uniformity of VHP concentration in the cabins. Case B (displacement delivery) had the most uniform decontaminant concentration distribution in both the cabins. Case C (delivery with mixing fans) had the least uniform distribution.

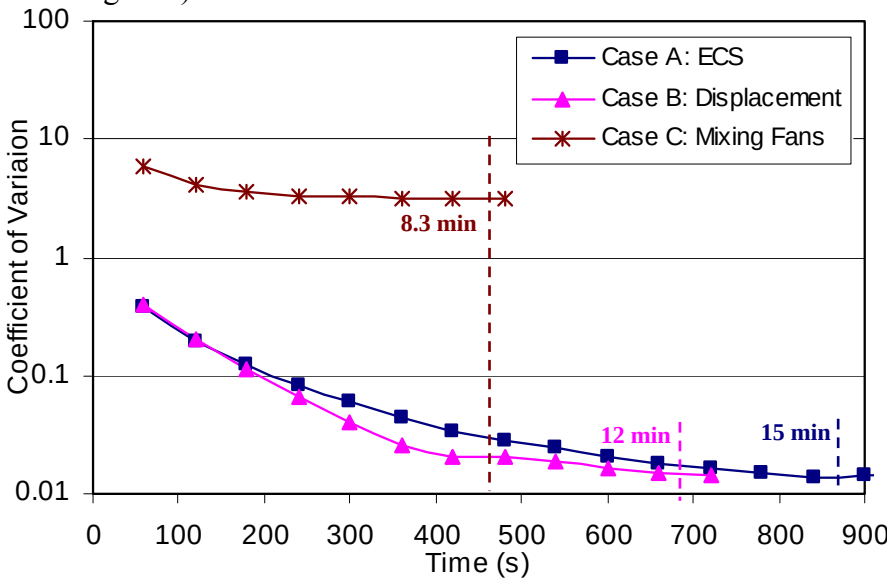

(a)

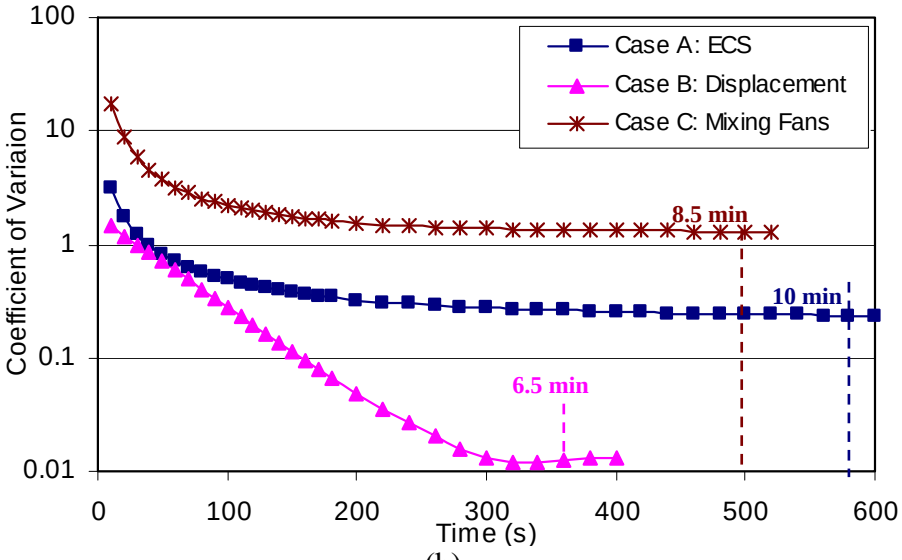

(b)

FIG. 9. Uniformity of VHP concentration distributions in (a) single-aisle cabin and (b) twin-aisle cabin.

The foremost important criterion in evaluating the sterilization efficacy is the rate of contaminant reduction. Figure 9 also shows the time needed to complete the sterilization. For the twin-aisle cabin, it took cases A, B, and C 10, 6.5 and 8.5 minutes, respectively, to complete the

sterilization as shown in Figure 9(b). Case B had clearly the best efficacy among the three. For the single-aisle cabin, Figure 9(a) shows that the sterilization process for cases A, B and C took 8.3, 12 and 15 minutes, respectively. The VHP distribution in case A was least uniform but the decontamination time is the shortest. Case B had the most uniform VHP distribution and moderate decontamination time. Case B was still regarded as the best one because the non-uniform distribution of VHP posed a high corrosion risk.

To prove such a risk, Figure 10 depicts the volume fraction with a VHP concentration exceeding 1000 ppm during the sterilization process. Case C in the single-aisle cabin had up to 4.3% of such volume fraction, because of the poor mixing of the VHP with the outside air before supplied into the cabin. Thereby, case C in the single-aisle cabin might not be safe even though it has the shortest sterilization process. That is why case B is regarded as the best one in both the cabins. Table 2 summarizes the performance of the three decontaminant delivery methods for the single-aisle and twin-aisle cabins.

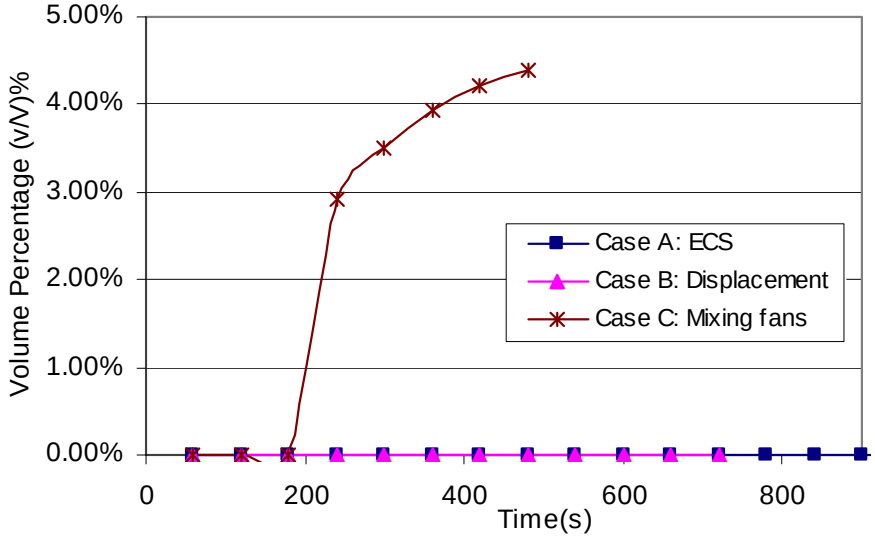

(a)

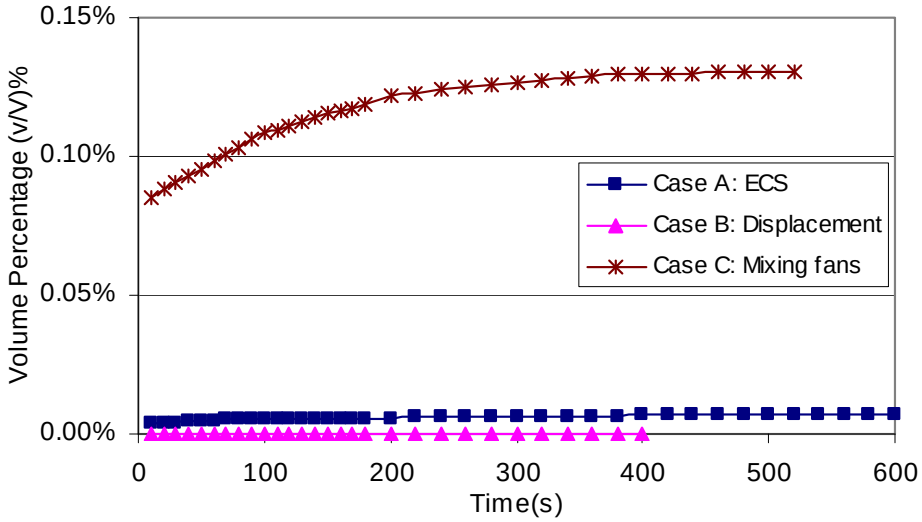

(b)

FIG. 10. Volume fraction with VHP concentration exceeding 1000ppm in (b) the single-aisle cabin and (b) the twin-aisle cabin.

TABLE 2. Summary of decontamination performance of three delivery methods

	Decontaminant delivery method	Sterilization speed	Uniformity	Corrosion risk
Single-aisle Cabin	Case A: ECS delivery	Slow	Good	Low
	Case B: Displacement delivery	Medium	Good	Low
	Case C: Delivery with mixing fans	Fast	Poor	Moderate
Twin-aisle Cabin	Case A: ECS delivery	Slow	Moderate	Low
	Case B: Displacement delivery	Fast	Good	Low
	Case C: Delivery with mixing fans	Medium	Poor	Moderate

4. Discussion

This paper used a CFD tool to identify the best decontaminant method in an aircraft cabin. Compared with the traditional experimental method, the CFD has several advantages. For example, it can easily change a delivery method. Should it be performed experimentally, the approach would be very expensive and time consuming. CFD can simulate a condition that may not easily be conducted in experiment, such as decontamination at a very high temperature and at a very low pressure. In addition, the numerical results are of great detail in a very fine resolution. Of course, CFD may not be accurate due to the approximations used. However, this can be remedy by validating the program with limited experimental data as shown in this paper.

This study modeled contaminant concentrations in air. The residual contamination is likely to be also on surfaces. Since the delivery of disinfectant to surfaces by using VHP is through the air, the VHP concentration in cells adjacent to the surfaces would be a good indicator for disinfection. Future study should include absorption, desorption and deposition of the disinfectant to surfaces.

It should be noted that the biological indicators used in the experimental studies cited in this paper were tri-pack stainless steel coupons inoculated with approximately 10^4, 10^5, and 10^6 CFU with *Geobacillus stearothermophilus* spores packaged in sub-divided Tyvek® envelopes. Rogers et al. [14] demonstrated that greater reduction in numbers on hard rather than porous surfaces. Considering most of material surface in an aircraft cabin is porous or soft surfaces, the surface effect deserves further study. In order to play safe, the disinfection time should be longer in actual decontaminantion processes in a cabin.

5. Conclusions

This study proposed a CFD method to study sterilization process for air cabin decontamination. The method was validated by using the measured air velocity and tracer-gas concentration in a cabin mockup and the tested decontamination efficacy in another cabin section obtained from the literature. The efficacy was indicated by using *Geobacillus stearothermophilus* spores on bio-indicators. The calculated results agreed reasonably with the two sets of experimental data. Thus, the CFD method is a viable tool to study decontamination processes in airliner cabins.

The validated CFD model was further used to investigate three VHP delivery methods in a single-aisle and a twin-aisle cabin. In order to identify an optimal delivery method, this study es the efficacy of sterilization process using the time to kill *Geobacillus stearothermophilus* spores, uniformity of the VHP concentration, and corrosion risk as evaluation criteria. The three methods were to delivery the VHP (1) through the ECS of the cabins, (2) through a front door and a back

door of the cabins by creating a displacement flow, and (3) in the cabins with many mixing fans. The second method with the displacement flow was the best because the decontamination time was moderate, the VHP distributions were most uniform, and the corrosion risk was low.

Acknowledgements

This project was funded by the U.S. Federal Aviation Administration (FAA) Office of Aerospace Medicine through the National Air Transportation Center of Excellence for Research in the Intermodal Transport Environment under Cooperative Agreement 07-C-RITE-PU. Although the FAA has sponsored this project, it neither endorses nor rejects the findings of this research. The presentation of this information is in the interest of invoking technical community comment on the results and conclusions of the research.

The authors wish to thank Dr. W. Gale of Auburn University and J. Thomas of Steris Corporation for supplying the data.

References

1. Block SS. Peroxygen compounds, In SS Block (ed.), Disinfection, sterilization and preservation, Lea and Febiger, Philadelphia, PA, 1991.
2. Chen X, Chen Q. Numerical investigation of decontaminant delivery strategies in a commercial aircraft cabin, Proceedings of the 10th International Conference on Air Distribution in Rooms (ROOMVENT 2007), Helsinki, Finland, 2007. p. 176,
3. Demeestere K, Dewulf J, De Witte B, Van Langenhove H. Titanium dioxide mediated heterogeneous photocatalytic degradation of gaseous dimethyl sulfide: Parameter study and reaction pathways, Applied Catalysis B: Environmental 2005;60:93-106.
4. Dionne JC, Soto JC, Pineau S. Assessment of an ultraviolet air sterilizer on the incidence of childhood upper respiratory tract infections and day care centre indoor air quality. Indoor Environment 1993;2:307-311.
5. Gale W. Private communications. Auburn University, AL. 2007.
6. Heckert RA, Best M, Jordan LT. Efficacy of vaporized hydrogen peroxide against exotic animal viruses. Applied and Environmental Microbiology 1997; 63:3916-3918.
7. Johnson JW, Arnold JF, Nail SF, Renzi E. Vaporized hydrogen peroxide sterilization of freeze dryers. Journal of Parenteral Science and Technology 1992;46:215–225.
8. Klapes NA, Vesley D. Vapor-phase hydrogen peroxide as a surface decontaminant and sterilant. Applied and Environmental Microbiology 1990; 56:503–506.
9. Mage DT, Ott WR. Accounting for nonuniform mixing and human exposure in indoor environments. BA Tichenor (ed.), Characterizing Sources of Indoor Air Pollution and Related Sink Effects, American Society for Testing and Materials, ASTM STP 1287. 1996. p. 263-278.
10. Menzies D, Pasztor JT, Rand J, Bourbeau J. Germicidal ultraviolet irradiation in air conditioning systems: effect on office worker health and wellbeing: a pilot study. Occup Environ Med 1999;56:397-402.
11. Morawska L. Droplet fate in indoor environments, or can we prevent the spread of infection? Indoor Air 2006;16: 335-347.
12. Raber E, McGuire R. Oxidative decontamination of chemical and biological warfare agents using L-Gel, Journal of Hazardous Materials 2002;93B:339-352.
13. Rickloff J, Orelski P. Resistance of various microorganisms to vapor phase hydrogen peroxide in a prototype dental hand piece/general instrument sterilizer, In Abstracts of the 89th Annual Meeting of the American Society for Microbiology. American Society for Microbiology, Washington, D.C. 1989.

14. Rogers JV, Sabourin CLK , Choi YW, Richter WR, Rudnicki DC , Riggs KB, Taylor ML, Chang J. Decontamination assessment of Bacillus an thracis, Bacillus subtilis, and Geobacillus stearothermophilus spores on indoor surfaces using a hydrogen peroxide gas generator. J ournal of Applied Microbiology 2005;99(4):739-748
15. Sekhar SC, Willem, HC. Impact of airflow profile on indoor air quality- a tropical study. Building and Environment 2004; 39:255-266.
16. Shaffstall RM, Garner RP, Bishop J, Cameron-Landi s L, Edding ton DL, Hau G, Spera S, Mielnik T, Thomas JA. Vaporized hydrogen pero xide (VHP®) decontamination of a section of a Boeing 747 cabin. Final Report. DOT/FAA/AM-06/10, Office of Aerospace Medicin e, Washington, DC. 2006.
17. Suen J, Alder man L, Kiley MP. Use of va por phase hy drogen peroxide (VPHP) a s a spac e decontaminant, In Progra m and abst racts of the ASM International S ymposium on Chem ical Germicides. American Society for Microbiology, Washington, D.C. 1990.
18. Thomas J. Cycle development guide. Internal Report. STERIS, Groveport, OH. 2007.
19. Yuan X, Chen Q, Glicksman LR. Models for prediction of temperature difference and ventilation effectiveness with displacement ventilation. ASHRAE Transactions 1999; 105(1):353-367.
20. Zhang Z, Zh ang W, Zhai Z, Chen Q. Evaluation of various turb ulence models in predicting airflow and turbulen ce in enclosed environm ents b y CFD: part-2: com parison with experimental data fro m literature, HVAC&R Research 2007;13(6):871-886.
21. Zhang Z, Chen X, Mazum dar S, Zhang T, Chen Q. Experimental and n umerical investigation of airflow and contam inant transport in an airlin er cabin m ockup, Buildin g and En vironment 200 9; 44:85-94.
22. Zhao J, Yang X. Photocataly tic oxidation for ind oor air purification: a literature review. Buil ding and Environment 2003;38:645-654.